J. Pharm. Pharmacol. 2000, 52: 273–280
Received June 10, 1999
Accepted November 9, 1999

Pharmacodynamics of S-2150, a Simultaneous Calcium-blocking and α_1-Inhibiting Antihypertensive Drug, in Rats

TORU ISHIBASHI, YOSHITAKA YANO AND TAKAYOSHI OGUMA

Developmental Research Laboratories, Shionogi & Co. Ltd, Sagisu 5-12-4, Fukushima-ku, Osaka 553-0002, Japan

Abstract

The in-vivo pharmacodynamics of S-2150, a newly developed dual-blocking type antihypertensive drug, was evaluated following intravenous infusion to rats. Previous in-vitro studies showed that the drug has two distinct mechanisms of antihypertensive effect—calcium-channel blocking activity and α_1-adrenoceptor antagonism—which could be explained by a combination of two different pharmacodynamic models.

The present in-vivo study showed that S-2150 also displays a complex pharmacodynamic profile (as measured by the decrease in mean blood pressure), which could be described by a combination of two sigmoid E_{max} models independently connected with the central compartment and the effect compartment.

These results suggested that the dual-blocking mechanism of S-2150, which has been observed in in-vitro experiments, was also evaluated by the pharmacodynamic analysis of in-vivo experimental data.

Safe, effective dosing design in pharmacotherapy requires understanding of the dose–effect relationship. An effect profile of a drug can be described by relating its pharmacokinetics for explanation of its concentration–time course profile with pharmacodynamics to explain the concentration–effect relationship (Holford & Sheiner 1981).

S-2150, a newly developed antihypertensive drug against ischaemia, is a 1,5-benzothiazepine derivative. Previous in-vitro studies (Kawakami et al 1996; Masui et al 1996; Kimoto et al 1997) have shown that this drug has both calcium-channel blocking activity and α_1-adrenoceptor antagonistic activity. However, the in-vivo pharmacodynamic profile of the drug has not been well examined, and it is not clear whether such dual-blocking mechanisms would actually be found in-vivo.

The pharmacodynamics of antihypertensive drugs in-vivo is usually evaluated by analysing the pharmacodynamic profile using an appropriate pharmacodynamic model (Harder et al 1992; Donnelly et al 1993). Because S-2150 has two distinct antihypertensive mechanisms, we planned to examine whether these two mechanisms would actually be reflected in the in-vivo pharmacodynamic profile of S-2150 and whether this profile could be described by a combination of two different pharmacodynamic models. To obtain basic information on the in-vivo pharmacodynamic effects of these two mechanisms, we used diltiazem and prazosin as reference drugs since they are typical of drugs acting by these mechanisms. The pharmacodynamic profile of S-2150 was independently evaluated from the results of pharmacodynamic analysis for diltiazem and prazosin. Problems were anticipated to arise from active metabolites produced after oral administration of S-2150 and diltiazem (Yabana et al 1985; Yeung et al 1990), which could make pharmacodynamic analysis difficult. Therefore we examined the pharmacodynamic properties of these drugs using intravenous infusion experiments in which only the pharmacodynamic effect of the unchanged form of the drug was considered.

Correspondence: T. Ishibashi, Developmental Research Laboratories, Shionogi & Co. Ltd, Sagisu 5-12-4, Fukushima-ku, Osaka 553-0002, Japan.
E-Mail: toru.ishibashi@shionogi.co.jp

Materials and Methods

Materials

S-2150 and deacetyl S-2150 were synthesized in Shionogi Research Laboratories (Osaka, Japan) as citrates. Diltiazem hydrochloride and prazosin hydrochloride were both purchased from Sigma

Chemical Co. (St Louis, MO). S-2150 and prazosin were dissolved in a mixture of 1·8% dimethylsulphoxide (DMSO) and 0·2% polyoxyethlene 60 hydrogenated castor oil (HCO-60) with saline. Diltiazem was dissolved in saline. DMSO was purchased from Wako Pure Chemical (Osaka, Japan) and HCO-60 was obtained from Nikko Chemicals (Tokyo, Japan). All other chemicals were of reagent grade.

Animal experiments

Male spontaneously hypertensive rats, 280–380 g, supplied by Shionogi Research Laboratories (Osaka, Japan) were used. To avoid the influence of blood sampling on blood pressure, the pharmacokinetic and pharmacodynamic experiments were performed with different groups of rats. On the day before the experiments, polyethylene cannulas (PE50, Nihon Becton-Dickinson, Tokyo, Japan) were placed in the left femoral vein for drug infusion, and in the right jugular vein (PE50) for blood sampling or in the left femoral artery (SP28, Natsume Seisakusho, Tokyo, Japan) for measurement of arterial blood pressure, under light ether anaesthesia.

With the rats conscious and allowed to move freely, S-2150 (6, 12 and 18 mg kg^{-1} h^{-1}), diltiazem (3, 6 and 12 mg kg^{-1} h^{-1}) and prazosin (0·02, 0·05 and 0·40 mg kg^{-1} h^{-1}) were infused intravenously for 30 min (total injection volume was 2 mL). Blood samples were collected at the end of the infusion and after another 5, 15, 30, 60 and 90 min, and were centrifuged immediately at 2000 *g* for 10 min. Plasma samples of 100 μL were kept frozen until assay by high-performance liquid chromatography (HPLC).

Only rats showing mean blood pressure (MBP) above 140 mmHg and systolic blood pressure above 175 mmHg were used for the pharmacodynamic experiments. Here, the MBP was obtained by calculating the mean of 500 measurements sampled at every 5 ms for 2·5 s. After a stabilization period of about 2 h, an infusion was started. MBP was measured every 30 s using a pressure transducer (TP-400T, Nihon Koden, Tokyo, Japan) and was recorded with a polygraph (RM-600, Nihon Koden, Tokyo, Japan) connected to a personal computer (PC-9801, NEC, Tokyo, Japan) for 2 h (diltiazem) or 12 h (S-2150 and prazosin). The change of MBP (E(%)) calculated by equation 1 was used as the index of the pharmacodynamic effect:

$$E(\%) = (MBP - MBP_0)/MBP_0 \times 100 \quad (1)$$

where E(%) is the change of MBP which is a measure of the antihypertensive effect and MBP_0 is the mean blood pressure for 30 min before the intravenous infusion of drugs.

Because we thought it fruitless to use all the measured MBP data for pharmacodynamic analysis, we sampled the MBP data from the measured data sets. The sampling intervals were 30 s for diltiazem; 1 min during infusion and 5 min after the infusion for prazosin; 1·5 min until 2 h after the infusion and 3 min thereafter for S-2150. The mean value of the change of MBP at each sampling time at each dosage was used for pharmacodynamic analysis. In all figures, to make the graphs clear, the mean values of the change of MBP were plotted for every three sampled points and the vertical bars for the standard deviation were not included. Instead, the range of C.V. (coefficient of variation) values are given in the results section.

MBP values in control experiments (i.e. no drug administered) were not affected by the infusion of the vehicle used for S-2150 and prazosin (data not shown).

HPLC assay of plasma drug concentration

Plasma concentrations of S-2150 and deacetyl S-2150, the main metabolite, were determined by HPLC. To 100 μL of plasma sample, 50 μL of methanol and 50 μL of 0·4 M acetate buffer (pH 4·1) with 10% methanol were added, followed by dilution with 300 μL of methanol. After mixing for 5 min, the mixture was centrifuged at 12 000 *g* for 5 min, then 50 μL of supernatant was injected into the HPLC system. The HPLC system (LC-6A, Shimadzu, Kyoto, Japan) was equipped with an ultraviolet detector (SPD-6A, Shimadzu, Kyoto, Japan) and was used with a stationary phase of J'sphere ODS-H80 (4·6 mm i.d. × 150 mm, YMC, Kyoto, Japan). The mobile phase, consisting of a mixture of 0·1% acetic acid with 10 mM sodium 1-octansulfonate and acetonitrile (50 : 50), was delivered at 0·8 mL min^{-1} at room temperature. The detector wavelength was set at 246 nm. The correlation coefficient of the calibration line was more than 0·999 in the measurement concentration range.

The plasma concentration of diltiazem was determined with some modifications of the reported HPLC method (Goebel & Kölle 1985; Yeung et al 1989). To 100 μL of plasma sample, 50 μL of 5 μg mL^{-1} propranolol as the internal standard and 50 μL of 2% ammonium carbonate were added, and then 2 mL of a mixture of hexane and isopropanol (98 : 2) were added. After mixing for 5 min, the sample was centrifuged at 12 000 *g* for 5 min. To

900 μL of supernatant, 200 μL of 0·005 N hydrochloride was added. After mixing for 5 min, the mixture was centrifuged at 12 000 *g* for 5 min, and 50 μL of the aqueous phase was injected into the HPLC-UV system. The system was the same as that for the assay of S-2150. The mobile phase consisted of a mixture of 0·01 M ammonium acetate, methanol and acetonitrile (40 : 35 : 25), and 0·01% triethylamine, with the pH adjusted to 7·6 using glacial acetic acid. The HPLC-UV system was operated at room temperature with a flow rate of 1·0 mL min^{-1}. The detector wavelength was set at 237 nm. The correlation coefficient of the calibration line was more than 0·999 in the measurement concentration range.

The plasma concentration of prazosin was determined by the fluorometric HPLC method according to the method of Fouda et al (1988), with some modifications. To 100 μL of the plasma sample, 300 μL of methanol was added and mixed for 5 min. Next, the mixture was centrifuged at 12 000 *g* for 5 min and 50 μL of the supernatant was injected into the HPLC system. The system was the same as that for the assay of S-2150 except for the column, a Capcell Pack 5C18 (4·6 mm i.d. × 150 mm, Shiseido, Tokyo, Japan), and the mobile phase, a mixture of 0·01 M phosphate buffer (pH 8·0), methanol and acetonitrile (65 : 15 : 20). The flow rate was 1·0 mL min^{-1}. The excitation and emission wavelengths were set at 246 and 389 nm, respectively, using a fluorescence detector (RF-535, Shimadzu, Kyoto, Japan). The correlation coefficient of the calibration line was more than 0·999 in the measurement concentration range.

Pharmacokinetic and pharmacodynamic analysis

The plasma concentration profiles of the three drugs were analysed by both one- and two-compartment models and the best model was selected according to the AIC (Akaike's information criterion) method (Akaike 1974; Yamaoka et al 1978). As shown below, the AIC estimation suggested that the two-compartment model could well describe the pharmacokinetic profiles of all 3 drugs, and we present here the model equations only for the two-compartment model.

During infusion:

$$Cp = \frac{Rate}{Vc(\alpha-\beta)}\left\{\frac{\alpha-k_{21}}{\alpha}(1-e^{-\alpha t}) + \frac{k_{21}-\beta}{\beta}(1-e^{-\beta t})\right\} \quad (2)$$

After infusion:

$$Cp = \frac{Rate}{Vc(\alpha-\beta)}\left\{\frac{\alpha-k_{21}}{\alpha}(e^{\alpha T}-1)e^{-\alpha t} + \frac{k_{21}-\beta}{\beta}(e^{\beta T}-1)e^{-\beta T}\right\} \quad (3)$$

$$\alpha+\beta = k_{12}+k_{21}+k_{10}$$
$$\alpha\cdot\beta = k_{21}\cdot k_{10}$$

In equations 2 and 3, Rate is the infusion rate, T is the infusion period, Vc is the distribution volume of the central compartment, k_{12} and k_{21} are the transfer rate constants between the compartments, k_{10} is the elimination rate constant and t is time after the start of infusion. The mean values of the plasma concentration data obtained from rats for each dose were simultaneously fitted by a two-compartment model using a nonlinear least-squares program NONLIN (Metzler et al 1974), and the refined parameters such as the total clearance (CL) and the half-life of the β-phase ($t_{\frac{1}{2}}(\beta)$), were also calculated. In the subsequent pharmacokinetic/pharmacodynamic analysis, the pharmacokinetic parameters were fixed at the estimated values, and the predicted drug concentration in plasma (central) compartment or the effect compartment (Sheiner et al 1979) at each time was used.

The pharmacodynamic model was selected from three candidates—the E_{max} (equation 4), the sigmoid E_{max} (equation 5) and the linear (equation 6) models:

$$E = E_0 - E_{max}\, C/(EC50 + C) \quad (4)$$

$$E = E_0 - E_{max}\, C^{\gamma}/(EC50^{\gamma} + C^{\gamma}) \quad (5)$$

$$E = E_0 - aC \quad (6)$$

where E is the change of MBP calculated by equation 1, E_0 is the base line (in this study, E_0 equals 0%), E_{max} is the maximum effect, C is the drug concentration, EC50 is the drug concentration required to produce 50% effect of E_{max}, γ is a parameter which determines the shape of the sigmoid curve and a is the slope of the response to the drug concentration. These pharmacodynamic models were linked to the pharmacokinetic models with or without the effect compartment. The mean value of the change of MBP at each sampling time at each dosage was simultaneously fitted by each combination of the pharmacodynamic models using NONLIN, and the best pharmacodynamic model was statistically selected based on the minimum AIC estimation method (Akaike 1974; Yamaoka et al 1978). The number of animals used are shown in each figure caption.

Results

Pharmacokinetics of diltiazem, prazosin and S-2150

Plasma concentration profiles of diltiazem, prazosin and S-2150 are shown in Figure 1 with the time-course curves predicted by the two-compartment model. The plasma concentration of deacetyl S-2150, the main metabolite was below the quantification limit in all samples. Although some peaks in the HPLC data might have been from a metabolite of diltiazem, they were all less than 10% of the peak area of the parent drug in the same sample. There were no peaks in the HPLC data which could

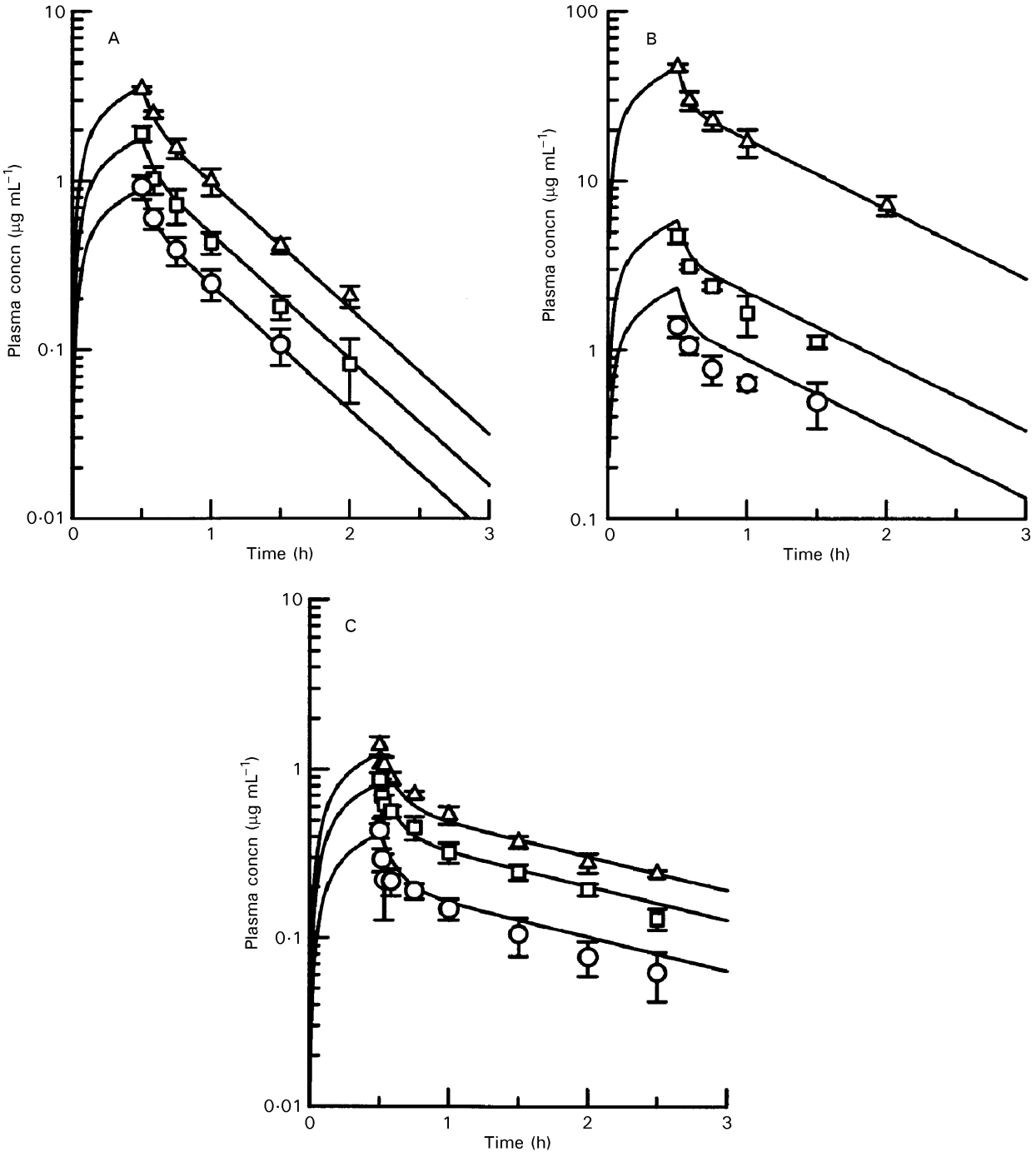

Figure 1. Plasma concentration profiles in spontaneously hypertensive rats after intravenous infusion of diltiazem (A), prazosin (B) and S-2150 (C). The curves represent the time-courses by the two-compartment model. Infusion rates of diltiazem: 3 (○), 6 (□) and 12 (△) mg kg^{-1} h^{-1} (n = 4–6); prazosin: 0·02 (○), 0·05 (□) and 0·4 (△) mg kg^{-1} h^{-1} (n = 3–6); S-2150: 6 (○), 12 (□) and 18 (△) mg kg^{-1} h^{-1} (n = 3–8). The data are shown as means ± s.d.

Table 1. Estimated pharmacokinetic parameters of diltiazem, prazosin and S-2150.

	Diltiazem	Prazosin	S-2150
k_{12} (h^{-1})	5·74 ± 0·56	11·4 ± 0·79	5·45 ± 1·00
k_{21} (h^{-1})	5·08 ± 0·38	3·94 ± 0·18	2·11 ± 0·20
k_{10} (h^{-1})	4·64 ± 0·32	4·54 ± 0·23	2·01 ± 0·20
V_c ($L\,kg^{-1}$)	0·45 ± 0·04	0·86 ± 0·05	1·90 ± 0·03
CL ($L\,h^{-1}$)	2·10	3·91	3·81
$t_{\frac{1}{2}}$ (β) (h)	0·40	0·73	1·49

have been from metabolites of prazosin. Comparison of the AIC values between the pharmacokinetic model candidates suggested that a two-compartment model would better describe the pharmacokinetic profiles of all the drugs under study. The pharmacokinetic parameters estimated by the two-compartment model are shown in Table 1.

Pharmacodynamics of diltiazem, prazosin, and S-2150

The plot of the change of MBP vs the plasma concentration after diltiazem infusion showed no hysteresis loop (data not shown) and suggested no time lag between the plasma concentration and MBP profiles. Therefore we linked each pharmacodynamic model (equations 4–6) to the central compartment and selected the best model by the minimum AIC estimation. The sigmoid E_{max} model gave the minimum AIC value and was selected to describe the pharmacodynamic profile after diltiazem infusion. The time-course profiles of the mean change of MBP are shown in Figure 2 with the curves obtained by the final pharmacodynamic model. The C.V. of MBP was in the range 0·3–15·8%. MBP decreased during infusion and recovered soon after the infusion terminated. MBP recovered almost up to the initial value (control value) within 2 h.

The relationship between the plasma concentration and the mean change of MBP with prazosin is shown in Figure 3, which shows clear hysteresis loops, and suggests the need to use the effect compartment. Therefore, we linked each pharmacodynamic model to the effect compartment. The sigmoid E_{max} model linked to the effect compartment gave the minimum AIC value and was selected to describe the pharmacodynamic profile after prazosin infusion. Time-course profiles of the mean change of MBP after prazosin infusion are shown in Figure 4 with the curves obtained by the final pharmacodynamic model. The C.V. of MBP was in the range 0·3–16·2%. MBP decreased during the infusion and recovered gradually after the end of infusion until 12 h. The final pharmacodynamic parameters of diltiazem and prazosin are shown in Table 2, where k_{e0} is the elimination rate constant from the effect compartment.

Time-course profiles of the mean change of MBP after S-2150 infusion are shown in Figure 5 with the curves obtained by the final pharmacodynamic model. The C.V. of MBP was in the range 0·4–8·5%. The change of MBP showed complicated profiles (i.e. MBP decreased rapidly during infusion, increased rapidly soon after the end of infusion and recovered slowly until 12 h). The plot of

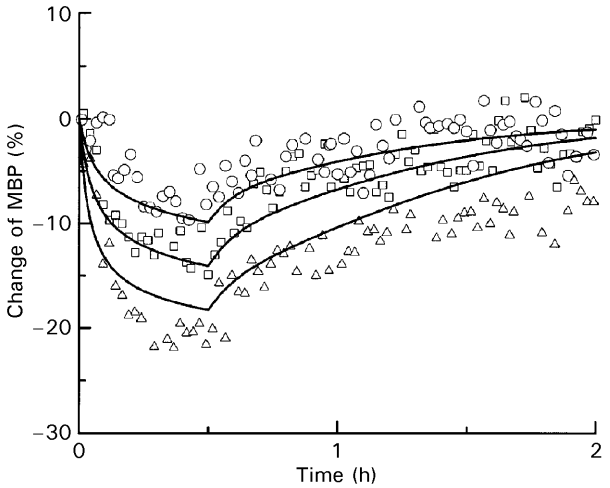

Figure 2. Time-course profile of the mean change of MBP after intravenous infusion of diltiazem to spontaneously hypertensive rats at a rate of 3 (○), 6 (□) or 12 (△) $mg\,kg^{-1}\,h^{-1}$. Each point represents the mean (n = 3–8). The curves represent the MBP profiles by the sigmoid E_{max} model connected with the central compartment.

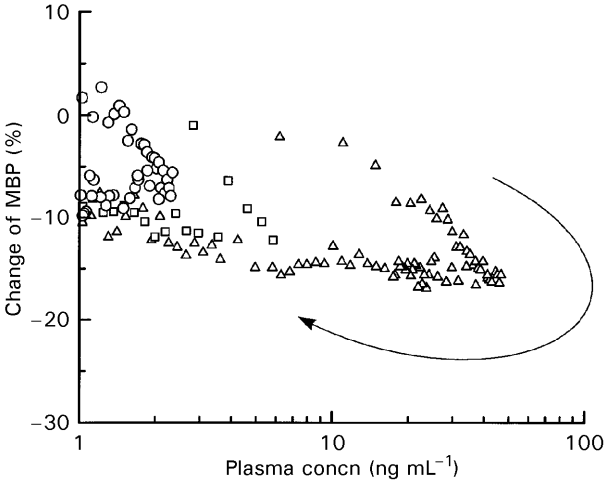

Figure 3. Relationship between calculated plasma concentration and the mean change of MBP after intravenous infusion of prazosin to spontaneously hypertensive rats at a rate of 0·02 (○), 0·05 (□) or 0·4 (△) $mg\,kg^{-1}\,h^{-1}$. Each point represents the mean value (n = 5–8). Plasma concentrations at the time of blood pressure measurements were calculated according to the two-compartment model parameters.

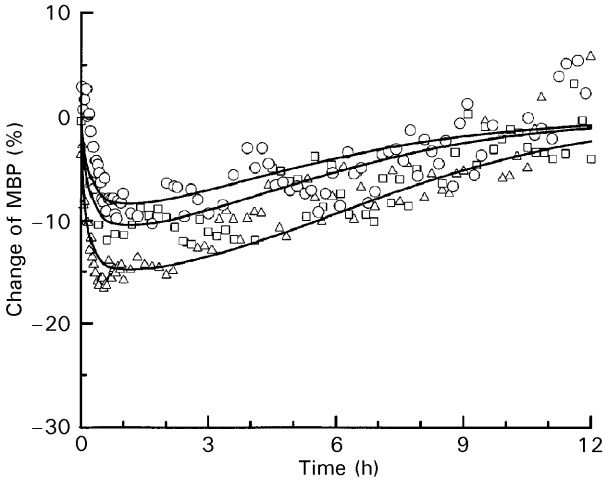

Figure 4. Time-course profile of the mean change of MBP after intravenous infusion of prazosin to spontaneously hypertensive rats at a rate of 0·02 (○), 0·05 (□) or 0·4 (△) mg kg^{-1} h^{-1}. Each point represents the mean (n = 5–8). The curves represent the MBP profiles by the sigmoid E_{max} model connected with the effect compartment.

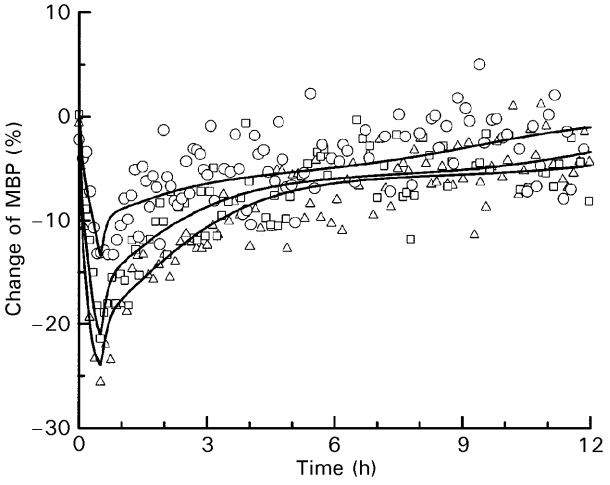

Figure 5. Time-course profile of the mean change of MBP after intravenous infusion of S-2150 to spontaneously hypertensive rats at a rate of 6 (○), 12 (□) or 18 (△) mg kg^{-1} h^{-1}. Each point represents the mean value (n = 8–12). The curves represent the MBP profiles by the combination of the sigmoid E_{max} models with the central compartment and the effect compartment (equation 6).

Table 2. Estimated final pharmacokinetic parameters of diltiazem and prazosin.

	Diltiazem[a]	Prazosin[b]
k_{e0} (h^{-1})	—	0·83 ± 0·05
E_{max} (%)	28·10 ± 0·05	23·00 ± 0·37
EC50 ($\mu g\,mL^{-1}$)	1·78 ± 0·08	$3{\cdot}17 \times 10^{-3} \pm 0{\cdot}20 \times 10^{-3}$
γ	0·89 ± 0·03	0·39 ± 0·02

[a]Linked to the central compartment. [b]Linked to the effect compartment.

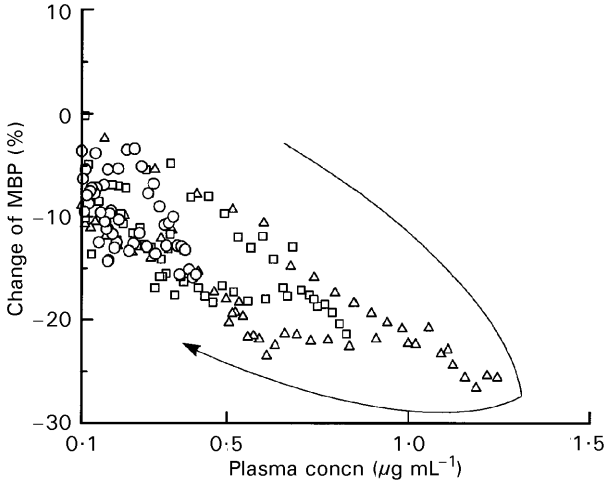

Figure 6. Relationship between calculated plasma concentration and the mean change of MBP after intravenous infusion of S-2150 to spontaneously hypertensive rats at a rate of 6 (○), 12 (□) or 18 (△) mg kg^{-1} h^{-1}. Each point represents the mean value (n = 8–12). Plasma concentrations at the time of blood pressure measurements were calculated according to the two-compartment model parameters.

change of MBP versus the plasma concentration also showed a hysteresis loops. The relationship between the plasma concentration and the mean change of MBP with S-2150 is shown in Figure 6, which shows hysteresis loops.

It may be difficult to compare the pharmacological effects of these three compounds because of the differences in their tissue distribution and pharmacological intensity. However, by comparing these results with those of the pharmacodynamic analysis of diltiazem and prazosin shown in Figures 2 and 4, and by considering the dual-type antihypertensive mechanism of S-2150, it seems possible to assume that the rapid recovery of MBP can be described by the pharmacodynamic model connected with the central compartment, and the slow recovery of MBP by the pharmacodynamic model connected with the effect compartment. Based on these assumptions, a plausible pharmacodynamic model for S-2150 was constructed by combining each pharmacodynamic model for diltiazem and prazosin, as given by equation 7:

$$E = E_0 - \left(\frac{E_{\max_{(Cp)}} \cdot Cp^{\gamma_{(Cp)}}}{EC_{50_{(Cp)}}^{\gamma_{(Cp)}} + Cp^{\gamma_{(Cp)}}} + \frac{E_{\max_{(Ce)}} \cdot Ce^{\gamma_{(Ce)}}}{EC_{50_{(Ce)}}^{\gamma_{(Ce)}} + Ce^{\gamma_{(Ce)}}} \right) \quad (7)$$

where Cp is plasma (central compartment) drug concentration and Ce is the hypothetical drug concentration in the effect compartment. Cp and Ce indicate that the pharmacodynamic model is connected with the central compartment or the effect compartment, respectively. The MBP data after S-

Table 3. Estimated final pharmacodynamic parameters of S-2150.

$E_{max(Cp)}$ (5)	23·0 ± 2·23
$EC50_{(Cp)}$ ($\mu g\,mL^{-1}$)	0·46 ± 0·06
$\gamma_{(Cp)}$	1·45 ± 0·14
k_{e0} (h^{-1})	0·22 ± 0·02
$E_{max(Ce)}$ (%)	5·60 ± 0·31
$EC50_{(Ce)}$ ($\mu g\,mL^{-1}$)	0·030 ± 0·002
$\gamma_{(Ce)}$	2·82 ± 0·50

2150 infusion were simultaneously fitted by the combined model (equation 7) To find the best pharmacodynamic model for S-2150 independently of the pharmacodynamic analysis of the other two drugs, other possible model candidates with various combinations of E_{max}, sigmoid E_{max}, and linear models and with or without the effect compartment were fitted to the same data set. According to the minimum AIC estimation, the results suggested that the pharmacodynamic model including both the sigmoid E_{max} model connected with the central compartment and the sigmoid E_{max} model connected with the effect compartment (i.e. the model given by equation 7) was the best for describing the complicated pharmacodynamic profiles after S-2150 infusion. This finding indicates that the pharmacodynamic profile of S-2150 can not be explained by a single pharmacodynamic model because of its complex antihypertensive mechanism, probably due to dual-blocking type activity. The pharmacodynamic parameters of S-2150 estimated by the final model are shown in Table 3.

Discussion

S-2150 is a newly developed antihypertensive drug with calcium-channel blocking activity but with less cardiodepressive activity (Masui et al 1996), and also has α_1-adrenoceptor antagonistic activity. In the present study, we performed a pharmacokinetic/pharmacodynamic analysis to examine the antihypertensive effects of S-2150 after intravenous infusion to spontaneously hypertensive rats to find whether such unique mechanisms also affect the in vivo pharmacodynamic profile. The results suggested that the pharmacodynamic effect of S-2150 could be well explained by the combination of two separate pharmacodynamic models (i.e. the sigmoid E_{max} models connected with the central compartment and with the effect compartment).

We measured the plasma concentration of S-2150 until 2 h after the infusion because of the detection limit. Therefore the above results are based on the assumption that the plasma–concentration profiles after the termination of concentration measurements can be extrapolated by the two-compartment model and the terminal half-life would not change. If the slower elimination phase (γ-phase) exists after 2 h, the pharmacodynamic parameter estimates may be different from those we showed. However, our conclusion that the pharmacodynamic profile of S-2150 can be explained by combination of the two pharmacodynamic models will not change because of the existence of the hysteresis loop at the concentration range above the detection limit (Figure 6).

As shown in Figure 2, the antihypertensive effect of diltiazem showed quick response to the change of plasma diltiazem concentration. Although the sigmoid E_{max} model was statistically selected for the pharmacodynamic model of diltiazem according to the AIC, the parameter γ was close to 1 which corresponds to the E_{max} model, and there were little differences in other parameters between these two pharmacodynamic models. Considering the variability of the MBP data, it does not seem very important to strictly distinguish between these two models.

The antihypertensive effect of prazosin in man showed a slow recovery compared with the plasma concentration profile, and the antihypertensive effect of prazosin has been explained by the pharmacodynamic model connected with the effect compartment (Elliott et al 1989). Pharmacodymamics of similar α_1-adrenoceptor antagonists, doxazosin and trimazosin, have also been analysed by the effect compartment model (Meredith et al 1983; Vincent et al 1983). Also, α_1-adrenoceptors have been reported to respond not to circulating noradrenaline but directly to neuronal control (Medgett & Langer 1984; van Zwieten et al 1988). This might be one of the reasons for the assumption of a time lag between the effect and the plasma concentration profiles, and the antihypertensive effect of the α_1-adrenoceptor antagonist being well described by using the effect compartment.

The antihypertensive effect of S-2150 was reported to be attenuated by prazosin pre-treatment under experimental conditions wherein the prazosin-induced decrease in blood pressure was compensated for by continuous intravenous infusion of angiotensin II in-vivo (Kawakami et al 1996). This suggests that the antihypertensive effect of S-2150 is caused partly by α_1-adrenoceptor antagonism in-vivo.

From the results of pharmacodynamic analyses of these three drugs, it seems reasonable to suppose that different mechanisms cause the rapid recovery of MBP explained by the pharmacodynamic model conected with the central compartment and the slow recovery of MBP explained by the pharmacodynamic model with the effect compartment.

In summary, after the infusion of S-2150 there was a rapid decrease in MBP followed by a rapid then slow recovery phase of MBP. By considering the pharmacodynamic profiles of the two reference drugs and the findings of the in-vitro studies, we explained that such a complex profile was caused by the dual-block type mechanisms of S-2150. We showed that the final pharmacodynamic model, consisting of two pharmacodynamic models, well described the antihypertensive profile of S-2150. A combination of two pharmacodynamic models has also been used by Paalzow & Edlund (1979) to describe the actions of clonidine. Our present study shows that in some cases, the pharmacodynamic effect of a drug may not be explainable by a simple pharmacodynamic model, and a more complex model may be required according to the pharmacological mechanisms of the drug.

Acknowledgements

The authors wish to thank Dr Kazumi Iwaki, Mr Tomoji Kawabata and Mr Masao Haruna in Shionogi Research Laboratories for their helpful suggestions in experimental techniques. We also thank Mr Kenji Shimamura and Mr Gakuji Kiyonaka in Shionogi Research Laboratories for their helpful assistance in this work.

References

Akaike, H. (1974) Stochastic theory of minimal realization. I.E.E.E. Trans. Automat. Contr. 19: 716–723

Donnelly, R., Meredith, P. A., Miller, S. H. K., Howie, C. A., Elliott, H. L. (1993) Pharmacodynamic modeling of the antihypertensive response to amlodipine. Clin. Pharmacol. Ther. 54: 303–310

Elliott, H. L., Donnelly, R., Meredith, P. A., Reid, J. L. (1989) Predictability of antihypertensive responsiveness and α-adrenoceptor antagonism during prazosin treatment. Clin. Pharmacol. Ther. 46: 576–583

Fouda, H. G., Twomey, T. M., Schneider, R. P. (1988) Liquid chromatographic analysis of doxazosin in human serum with manual and robotic sample preparation. J. Chromatogr. Sci. 26: 570–573

Goebel, K. J., Kölle, E. U. (1985) High-performance liquid chromatographic determination of diltiazem and four of its metabolites in plasma: application to pharmacokinetics. J. Chromatogr. 345: 355–363

Harder, S., Thürmann, P., Siewert, M., Blume, H., Rietbrock, N., van der Kleijn, J., Gierend, M. (1992) Concentration/effect relationship and enantioselective analysis of verapamil in hypertensive patients. J. Cardiovasc. Pharmacol. 19: 665–669

Holford, N. H. G., Sheiner, L. B. (1981) Understanding the dose-effect relationship: clinical application of pharmacokinetic-pharmacodynamic models. Clin. Pharmacokinet. 6: 429–453

Kawakami, M., Matsumura, S., Shimamura, T., Iwasaki, T., Furukawa, H., Matsunaga, K., Yonetani, Y., Iwaki, K. (1996) Pharmacological studies on a new antihypertensive agent, S-2150, a benzothiazepine derivative: 2. Hypotensive effects in normotensive and hypertensive rats. J. Cardiovasc. Pharmacol. 28: 695–702

Kimoto, S., Haruna, M., Matsuura, E., Uno, O., Ishii, M., Hirono, S., Yoshimura, K., Ueda, M., Iwaki, K. (1997) Pharmacological studies on a new antihypertensive agent, S-2150, a benzothiazepine derivative: 3. Hypotensive and antimyocardial-stunning effects in dogs. J. Cardiovasc. Pharmacol. 29: 180–187

Masui, M., Funakawa, S., Uno, O., Mihara, S., Takahara, Y., Matsunaga, K., Iwaki, K. (1996) Pharmacological studies on a new antihypertensive agent, S-2150, a benzothiazepine derivative: 1. Antinecrotic and antiarrhythmic effects in reperfused rat hearts. J. Cardiovasc. Pharmacol. 28: 526–532

Medgett, I. C., Langer, S. Z. (1984) Heterogeneity of smooth muscle alpha adrenoceptors in rat tail artery in vitro. J. Pharmacol. Exp. Ther. 229: 823–830

Meredith, P. A., Kelman, A. W., Elliot, H. L., Reid, J. L. (1983) Pharmacokinetic and pharmacodynamic modelling of trimazosin and its major metabolite. J. Pharmacokinet. Biopharm. 11: 323–335

Metzler, C. M., Elfring, G. K., McEwen, A. J. (1974) A package of computer programs for pharmacokinetic modeling. Biometrics 30: 562–563

Paalzow, L. K., Edlund, P. O. (1979) Multiple receptor responses: a new concept to describe the relationship between pharmacological effects and pharmacokinetics of a drug: studies on clonidine in the rat and cat. J. Pharmacokinet. Biopharm. 7: 495–510

Sheiner, L. B., Stanski, D. R., Vozeh, S., Miller, R. D., Ham, J. (1979) Simultaneous modeling of pharmacokinetics and pharmacodynamics: application to d-tubocurarine. Clin. Pharmacol. Ther. 25: 358–371

Van Zwieten, P. A. (1988) Antihypertensive drugs interacting with α- and β-adrenoceptors: a review of basic pharmacology. Drugs 35 (Suppl. 6): 6–19

Vincent, J., Elliot, H. L., Meredith, P. A., Reid, J. L. (1983) Doxazosin, an alpha1-adrenoceptor antagonist: pharmacokinetics and concentration-effect relationships in man. Br. J. Clin. Pharmacol. 15: 719–725

Yabana, H., Nagao, T., Sato, M. (1985) Cardiovascular effects of the metabolites of diltiazem in dogs. J. Cardiovasc. Pharmacol. 7: 152–157

Yamaoka, K., Nakagawa, T., Uno, T. (1978) Application of Akaike's information criterion (AIC) in the evaluation of linear pharmacokinetic equations. J. Pharmacokinet. Biopharm. 6: 165–175

Yeung, P. K. F., Montague, T. J., Tsui, B., McGregor, C. (1989) High-performance liquid chromatographic assay of diltiazem and six of its metabolites in plasma: application to a pharmacokinetic study in healthy volunteers. J. Pharm. Sci. 78: 592–597

Yeung, P. K. F., Mosher, S. J., Quilliam, M. A., Montague, T. J. (1990) Species comparison of pharmacokinetics and metabolism of diltiazem in humans, dogs, rabbits, and rats. Drug Metab. Dispos. 18: 1055–1059